

# $\tau \rightarrow \omega 3\pi \nu$ Decays

Jun Gao and Bing An Li

Department of Physics and Astronomy, University of Kentucky

Lexington, KY 40506, USA

## Abstract

Theoretical study of anomalous decay mode  $\tau \rightarrow \omega \pi \pi \pi \nu$  is presented. Theoretical value of the branching ratio of  $\tau^- \rightarrow \omega \pi^- \pi^0 \pi^0 \nu$  agrees well with data. The branching ratio of  $\tau^- \rightarrow \omega \pi^+ \pi^- \pi^- \nu_\tau$  is predicted. It is found that the vertices of  $a_1 \rho \pi$  and  $\omega \rho \pi$  play dominant role in these two decay modes. CVC is satisfied and there is no adjustable parameter.

There is rich physics in  $\tau$  hadronic decays. Because of the value of  $m_\tau$  many light mesons made of u, d, and s quarks, especially meson resonances, are produced in the decays. Therefore,  $\tau$  mesonic decays provide very unique test ground of Standard Model and QCD. An effective theory of large  $N_C$  QCD of mesons has been proposed to study the physics of light mesons [1]. In this theory the tree diagrams of mesons are at leading order of large  $N_C$  expansion and loop diagrams are at higher orders. This theory has been applied to study many physical processes of mesons and it has been shown that the theory is phenomenologically successful [1, 2, 3]. Both vector and axial-vector currents contribute to  $\tau$  decays. The mesonic vector current is obtained from the Vector Meson Dominance(VMD) which is a natural result of this theory [1]. The axial-vector current of mesons is also obtained [3]. PCAC is satisfied[3]. Many  $\tau$  mesonic decay modes have been studied by using this theory [3]. Theory agrees with data reasonably well.

The decay rate of  $\tau^- \rightarrow 2\pi^-\pi^+3\pi^0\nu_\tau$  has been measured by ALEPH [4] and CLEO [5] and predicted by CVC [6, 7, 8]. The first measurement of  $\tau^- \rightarrow \omega\pi^-\pi^0\pi^0\nu_\tau$  has been reported by CLEO [5]

$$B(\tau^- \rightarrow \omega\pi^-\pi^0\pi^0\nu_\tau) = (1.89_{-0.67}^{+0.74} \pm 0.40) \times 10^{-4}.$$

There is another decay mode  $\tau^- \rightarrow \omega\pi^+\pi^-\pi^-\nu_\tau$ . They are very interesting decay modes which are resulted from the vector current. These decay modes are tests of VMD.  $\omega$  meson is associated with anomaly. Wess-Zumino-Witten anomaly [9] can be tested by these modes.

Since four mesons are produced, many meson vertices are involved in these processes. These decay modes provide tests on all kinds of meson theory. In the effective theory of large  $N_C$  QCD of mesons [1] all the vertices of these decays have been derived and all the parameters have been fixed. The large  $N_C$  theory of mesons [1] will make definite predictions on these two decay modes. Therefore, they provide serious tests on this theory.

In this paper we apply the effective theory of large  $N_C$  QCD [1] to study  $\tau^- \rightarrow \omega\pi^-\pi^0\pi^0\nu_\tau$  and  $\tau^- \rightarrow \omega\pi^+\pi^-\pi^-\nu_\tau$ . Only vector current contributes to both decays, which has been derived as [3]

$$\mathcal{L}^V = \frac{g_W}{4}\cos\theta_C g \left\{ -\frac{1}{2}(\partial_\mu A_\nu^i - \partial_\nu A_\mu^i)(\partial^\mu \rho^{i\nu} - \partial^\nu \rho^{i\mu}) + A_\mu^i j^{i\mu} \right\}, \quad (1)$$

where  $A_\mu^i$  is the W boson field,  $j_\mu^i$  is derived by the substitution

$$\rho_\mu^i \rightarrow \frac{g_W}{4} g \cos\theta_C A_\mu^i \quad (2)$$

in the vertices involving  $\rho$  meson and  $g$  is a universal coupling constant which is determined to be 0.39 by fitting  $\rho \rightarrow ee^+$ . Eq.(1) is exactly the same expression of VMD given by Sakurai [10].

The diagrams contributing to the decay  $\tau \rightarrow \omega\pi\pi\pi\nu$  are shown in Fig.1(a, b, c, d, e, f). All the vertices are derived in the chiral limit. The  $\omega\rho\pi$  vertex is the Wess-Zumino-Witten anomaly and derived as

$$\mathcal{L}^{\omega\rho\pi} = -\frac{3}{\pi^2 g^2 f_\pi} \epsilon^{\mu\nu\alpha\beta} \partial_\mu \omega_\nu \rho_\alpha^i \partial_\beta \pi^i. \quad (3)$$

The vertex  $\mathcal{L}^{\omega\rho\pi}$  leads to the Adler-Bell-Jackiw anomaly of  $\pi^0 \rightarrow \gamma\gamma$  [1].

Besides the anomalous vertices  $\mathcal{L}^{\omega\rho\pi}$ , there are other three kinds of normal vertices in Fig.1. The first kind of vertices derived in Ref.[1] are

$$\mathcal{L}^{a_1\rho\pi} = \epsilon_{ijk}\{A(q^2, p^2)a_\mu^i\rho^{j\mu}\pi^k - Ba_\mu^i\rho_\nu^j\partial^{\mu\nu}\pi^k + Da_\mu^i\partial^\mu(\rho_\nu^j\partial^\nu\pi^k)\}, \quad (4)$$

$$\begin{aligned} \mathcal{L}^{\rho\pi\pi} = & \frac{2}{g}\epsilon_{ijk}\rho_\mu^i\pi^j\partial^\mu\pi^k - \frac{2}{\pi^2 f_\pi^2 g}\{(1 - \frac{2c}{g})^2 - 4\pi^2 c^2\}\epsilon_{ijk}\rho_\mu^i\partial_\nu\pi^j\partial^{\mu\nu}\pi^k \\ & - \frac{1}{\pi^2 f_\pi^2 g}\{3(1 - \frac{2c}{g})^2 + 1 - \frac{2c}{g} - 8\pi^2 c^2\}\epsilon_{ijk}\rho_\mu^i\pi_j\partial^2\partial_\mu\pi_k, \end{aligned} \quad (5)$$

$$\mathcal{L}^{\rho\rho\rho} = -\frac{2}{g}\epsilon_{ijk}\partial_\mu\rho_\nu^i\rho^{j\mu}\rho^{k\nu}, \quad (6)$$

where

$$c = \frac{f_\pi^2}{2gm_\rho^2},$$

$$F^2 = (1 - \frac{2c}{g})^{-1}f_\pi^2,$$

$$\begin{aligned} A(q^2, p^2) = & \frac{2}{f_\pi}f_a\{\frac{F^2}{g^2} + p^2[\frac{2c}{g} + \frac{3}{4\pi^2 g^2}(1 - \frac{2c}{g})] \\ & + q^2[\frac{1}{2\pi^2 g^2} - \frac{2c}{g} - \frac{3}{4\pi^2 g^2}(1 - \frac{2c}{g})]\}, \end{aligned} \quad (7)$$

$$f_a = (1 - \frac{1}{2\pi^2 g^2})^{-\frac{1}{2}}, \quad (8)$$

$$B = -\frac{2}{f_\pi}f_a\frac{1}{2\pi^2 g^2}(1 - \frac{2c}{g}), \quad (9)$$

$$D = -\frac{2}{f_\pi}f_a\{\frac{2c}{g} + \frac{3}{2\pi^2 g^2}(1 - \frac{2c}{g})\} \quad (10)$$

with q being the momentum of  $a_1$  meson and p the momentum of  $\rho$  meson.

The vertices of  $\mathcal{L}^{a_1\rho\pi}$  and  $\mathcal{L}^{\rho\pi\pi}$  have been tested by the widths of  $a_1$  and  $\rho$ , pion form factors, and other physical processes [1, 2, 3]. Theory agrees well with data.

The second kind of normal vertices are contact interactions between two meson fields

$$\mathcal{L}^{\pi\pi} = \frac{1}{4\pi^2 f_\pi^2} \left(1 - \frac{2c}{g}\right)^2 \partial_{\mu\nu} \pi^i \partial^{\mu\nu} \pi^i, \quad (11)$$

$$\mathcal{L}^{\pi a} = \frac{f_a}{2\pi^2 g f_\pi} \left(1 - \frac{2c}{g}\right) \partial_{\mu\nu} \pi^i \partial^\mu a^{i\nu}, \quad (12)$$

$$\mathcal{L}^{aa} = \frac{f_a^2}{4\pi^2 g^2} (\partial_\mu a^{i\mu})^2. \quad (13)$$

By inserting these vertices into Fig.1(b, c), related diagrams are obtained.

The third kind of vertex is the direct interaction between  $\rho\rho\pi\pi$

$$\begin{aligned} \mathcal{L}^{\pi\pi\rho\rho} = & \frac{4}{f_\pi} \epsilon_{ijk} \epsilon_{ij'k'} \left\{ \frac{F^2}{2g^2} \rho_\mu^j \rho_\mu^{j'} \pi_k \pi_{k'} + \left[ -\frac{2c^2}{g^2} + \frac{3}{4\pi^2 g^2} \left(1 - \frac{2c}{g}\right)^2 \right] \rho_\mu^j \rho_\nu^{j'} \partial^\mu \pi_k \partial^\nu \pi_{k'} \right. \\ & + \left[ -\frac{2c^2}{g^2} + \frac{1}{4\pi^2 g^2} \left(1 - \frac{2c}{g}\right)^2 \right] \rho_\nu^i \rho^{j'\nu} \partial_\mu \pi_k \partial^\mu \pi_{k'} - \frac{2c^2}{g^2} \rho_\mu^j \rho_\nu^{k'} \partial^\nu \pi_k \partial^\mu \pi_{j'} \\ & - \frac{3}{2\pi^2 g^2} \left(1 - \frac{2c}{g}\right) (\rho_\mu^j \pi_k \partial_\nu \pi_{j'} - \rho_\nu^j \pi_k \partial_\mu \pi_{j'}) \partial^\nu \rho^{k'\mu} - \frac{1}{2\pi^2 g^2} \left(1 - \frac{2c}{g}\right) \rho_\mu^j \pi_k \rho_\nu^{j'} \partial^{\mu\nu} \pi_{k'} \\ & \left. + \frac{1}{4\pi^2 g^2} [\partial_\nu (\rho_\mu^j \pi_k) \partial^\nu (\rho_\mu^j \pi_{k'}) + 2 \left(1 - \frac{2c}{g}\right) \rho_\mu^j \pi_k \rho_\nu^{j'} \partial^{\mu\nu} \pi_{k'}] \right\}. \quad (14) \end{aligned}$$

This is the vertex of Fig.1(a).

Due to the structure of the vertex (1) the amplitudes of the diagrams Fig.1(e, f) satisfy the CVC automatically. However, for the diagrams(Fig.1(a, b, c, d)) we have to put all the three kinds of vertices(4-6, 11-14) together to make CVC be satisfied in the chiral limit. These vertices have been exploited to calculate the branching ratios of  $\tau \rightarrow \rho\pi\pi\nu$  [11]. Theoretical

results are in agreement with the data. It is necessary to emphasize that all the parameters of this study have been fixed in previous studies. There is no adjustable parameter in this investigation.

In diagram Fig.1(e) there are two anomalous vertices  $\mathcal{L}^{\omega\rho\pi}$ . The study [1] shows that the strength of this vertex is weaker than normal vertices. This is the reason why  $\omega$  meson has narrower decay width than  $\rho$  meson. The calculation shows that the contribution of diagram Fig.1(e) is negligible. In the diagram Fig.1(f) there are  $\rho$  resonance,  $\omega$  and  $\pi$  mesons in the final state. Because the phase space of this process is too small the contribution of this diagram is also negligible.

Now we calculate the branching ratios of  $\tau \rightarrow \omega\pi\pi\pi\nu$ . It is very lengthy. The amplitudes of the decays  $\tau \rightarrow \omega\pi\pi\pi\nu$  are obtained from all the three kinds of vertices(4-6, 11-14) and the vertex  $\mathcal{L}^{\omega\rho\pi}$  (3). In the chiral limit the matrix elements of the vector current of  $\tau^- \rightarrow \omega\pi^-\pi^0\pi^0\nu_\tau$  and  $\tau^- \rightarrow \omega\pi^+\pi^-\pi^-\nu_\tau$  have been derived as

$$\begin{aligned}
& \langle \omega(p)\pi^0(p_1)\pi^0(p_2)\pi^-(p_3) | j^{\mu-} | 0 \rangle \\
&= \frac{1}{\sqrt{16E\omega_1\omega_2\omega_3}} \left( g^{\mu\lambda} - \frac{q^\mu q^\lambda}{q^2} \right) \frac{3}{\pi^2 g f_\pi} \frac{-m_\rho^2 + i\sqrt{q^2}\Gamma_\rho(q^2)}{q^2 - m_\rho^2 + i\sqrt{q^2}\Gamma_\rho(q^2)} f_\lambda^{00}, \\
& f_\lambda^{00} = \epsilon_{\nu'\mu'} \varepsilon^{\mu'\nu'\alpha\beta} \\
& \left\{ \frac{p_{3\beta}}{(p+p_3)^2 - m_\rho^2 + i\sqrt{(p+p_3)^2}\Gamma_\rho((p+p_3)^2)} (f_{\alpha\lambda}^{(12)}(p+p_3) + f_{\alpha\lambda}^{(21)}(p+p_3)) \right. \\
& \left. - \frac{p_{1\beta}}{(p+p_1)^2 - m_\rho^2 + i\sqrt{(p+p_1)^2}\Gamma_\rho((p+p_1)^2)} f_{\alpha\lambda}^{(23)}(p+p_1) \right\}
\end{aligned} \tag{15}$$

$$-\frac{p_{2\beta}}{(p+p_2)^2 - m_\rho^2 + i\sqrt{(p+p_2)^2}\Gamma_\rho((p+p_2)^2)}f_{\alpha\lambda}^{(13)}(p+p_2)\}; \quad (16)$$

$$\begin{aligned} &< \omega(p)\pi^+(p_2)\pi^-(p_1)\pi^-(p_3) | j^{\mu-} | 0 > \\ &= \frac{1}{\sqrt{16E\omega_1\omega_2\omega_3}}(g^{\mu\lambda} - \frac{q^\mu q^\lambda}{q^2})\frac{3}{\pi^2 g f_\pi} \frac{-m_\rho^2 + i\sqrt{q^2}\Gamma_\rho(q^2)}{q^2 - m_\rho^2 + i\sqrt{q^2}\Gamma_\rho(q^2)}f_\lambda^{--}, \end{aligned} \quad (17)$$

$$f_\lambda^{--} = \epsilon_{\nu'} p_{\mu'} \varepsilon^{\mu'\nu'\alpha\beta}$$

$$\begin{aligned} &\{ \frac{p_{3\beta}}{(p+p_3)^2 - m_\rho^2 + i\sqrt{(p+p_3)^2}\Gamma_\rho((p+p_3)^2)}f_{\alpha\lambda}^{(12)}(p+p_3) \\ &+ \frac{p_{1\beta}}{(p+p_1)^2 - m_\rho^2 + i\sqrt{(p+p_1)^2}\Gamma_\rho((p+p_1)^2)}f_{\alpha\lambda}^{(32)}(p+p_1) \\ &- \frac{p_{2\beta}}{(p+p_2)^2 - m_\rho^2 + i\sqrt{(p+p_2)^2}\Gamma_\rho((p+p_2)^2)}(f_{\alpha\lambda}^{(13)}(p+p_2) + f_{\alpha\lambda}^{(31)}(p+p_2)) \}, \end{aligned} \quad (18)$$

where

$$q = p + p_1 + p_2 + p_3, \quad (19)$$

$$\begin{aligned} f_{\alpha\lambda}^{(12)}(p_\rho) &= g_{\alpha\lambda}f(p_\rho) + p_{1\alpha}[f_{11}(p_\rho)p_{1\lambda} + f_{21}(p_\rho)p_{2\lambda}] \\ &+ p_{2\alpha}[f_{12}(p_\rho)p_{1\lambda} + f_{22}(p_\rho)p_{2\lambda}] \end{aligned} \quad (20)$$

with  $p_\rho$  being the momentum of the  $\rho$  meson,  $p_i$  ( $i = 1, 2, 3$ ) the momentum of pion, and  $p$  the momentum of  $\omega$ .  $f_{\alpha\lambda}^{(21)}$  is obtained from  $f_{\alpha\lambda}^{(12)}$  by exchanging  $p_1 \leftrightarrow p_2$ ;  $f_{\alpha\lambda}^{(23)}$  is obtained from  $f_{\alpha\lambda}^{(21)}$  by replacing  $p_1$  with  $p_3$ ;  $f_{\alpha\lambda}^{(13)}$  is obtained from  $f_{\alpha\lambda}^{(12)}$  by replacing  $p_2$  with  $p_3$ ;  $f_{\alpha\lambda}^{(32)}$  is obtained from  $f_{\alpha\lambda}^{(23)}$  by exchanging  $p_2 \leftrightarrow p_3$ ;  $f_{\alpha\lambda}^{(31)}$  is obtained from  $f_{\alpha\lambda}^{(13)}$  by exchanging

$p_1 \leftrightarrow p_3$ .  $\Gamma_\rho$  is the decay width of  $\rho$  meson of momentum  $q$

$$\Gamma_\rho(q^2) = \frac{\sqrt{q^2}}{12\pi g^2} \left\{ 1 + \frac{q^2}{2\pi^2 f_\pi^2} \left[ \left( 1 - \frac{2c}{g} \right)^2 - 4\pi^2 c^2 \right] \right\}^2 \left( 1 - \frac{4m_\pi^2}{q^2} \right)^{\frac{3}{2}}. \quad (21)$$

Eqs.(15, 17) show that the CVC, indeed, is satisfied in the chiral limit. It is interesting to notice that the resonance factor

$$\frac{-m_\rho^2 + i\sqrt{q^2}\Gamma_\rho(q^2)}{q^2 - m_\rho^2 + i\sqrt{q^2}\Gamma_\rho(q^2)}$$

in Eqs.(15, 17) is obtained from the combination of the two terms in Eq.(1). These two terms are shown in two diagrams of Fig.1(a, b, c, d, e, f).

The contributions of  $a_1$  meson (Fig.1(b)) to the functions  $f$  and  $f_{ij}$  ( $i, j = 1, 2$ ) are given below. The contributions from other diagrams are shown in the appendix.

$$\begin{aligned} BW(k_1^2) &= \frac{1}{k_1^2 - m_a^2 + i\sqrt{k_1^2}\Gamma_a(k_1^2)}, \\ f(p_\rho) &= BW(k_1^2)A(q^2, k_1^2)A(p_\rho^2, k_1^2), \\ f_{11}(p_\rho) &= BW(k_1^2)A(p_\rho^2, k_1^2)B, \\ f_{12}(p_\rho) &= BW(k_1^2)\{[A(p_\rho^2, k_1^2) + A(q^2, k_1^2)]D + (k_1 \cdot p_2 - k_1 \cdot p_1)BD + p_1 \cdot p_2 B^2 - k_1^2 D^2\} \\ &\quad - BW(k_1^2)\frac{1}{m_a^2}\{-A(q^2, k_1^2) + k_1 \cdot p_1 B + k_1^2 D\}\{A(p_\rho^2, k_1^2) + k_1 \cdot p_2 B - k_1^2 D\}, \\ f_{22}(p_\rho) &= BW(k_1^2)A(q^2, k_1^2)B, \end{aligned} \quad (22)$$

where  $k_i = q - p_i$  ( $i = 1, 2, 3$ ) and

$$m_a^2 = \left( \frac{F^2}{g^2} + m_\rho^2 \right) / \left( 1 - \frac{1}{2\pi^2 g^2} \right). \quad (23)$$



The decay width of  $a_1$  meson is derived as

$$\begin{aligned}
\Gamma_a(k^2) &= \frac{k_a}{12\pi} \frac{1}{k^2} \left\{ \left(3 + \frac{k_a^2}{m_\rho^2}\right) A^2(m_\rho^2, k^2) \right. \\
&\quad \left. - A(m_\rho^2, k^2) B(k^2 + m_\rho^2) \frac{k_a^2}{m_\rho^2} + \frac{k^2}{m_\rho^2} k_a^4 B^2 \right\}, \\
k_a^2 &= \frac{1}{4k^2} (k^2 + m_\rho^2 - m_\pi^2)^2 - m_\rho^2.
\end{aligned} \tag{24}$$

The decay rate of  $\tau \rightarrow \omega \pi \pi \pi \nu$  is derived from Eqs.(15-18)

$$\frac{d\Gamma^{ab}}{dq^2} = \frac{1}{128} \frac{G^2}{(2\pi)^8} \cos^2 \theta_c \frac{1}{q^2} \frac{1}{m_\tau^3} (m_\tau^2 - q^2)^2 (m_\tau^2 + 2q^2) \left( \frac{3}{\pi^2 g f_\pi} \right)^2 \frac{m_\rho^4 + q^2 \Gamma_\rho^2(q^2)}{(q^2 - m_\rho^2)^2 + q^2 \Gamma_\rho^2(q^2)} F^{ab}(q^2), \tag{25}$$

where

$$ab = 00 \text{ or } --,$$

$$F^{ab}(q^2) = \frac{1}{3} (g^{\lambda\lambda'} - \frac{q^\lambda q^{\lambda'}}{q^2}) \frac{1}{4(2\pi)^2} \int \frac{d^3 p_1 d^3 p_2 d^3 p_3 d^3 p}{E \omega_1 \omega_2 \omega_3} \delta(q - p_1 - p_2 - p_3 - p) f_\lambda^{ab} f_{\lambda'}^{*ab}. \tag{26}$$

The branching ratios of the two decay channels are calculated to be

$$B(\tau^- \rightarrow \omega \pi^- \pi^0 \pi^0 \nu_\tau) = 2.16 \times 10^{-4}, \tag{27}$$

$$B(\tau^- \rightarrow \omega \pi^+ \pi^- \pi^- \nu_\tau) = 2.18 \times 10^{-4}. \tag{28}$$

Theoretical branching ratio of  $\tau^- \rightarrow \omega \pi^- \pi^0 \pi^0 \nu_\tau$  is consistent with the data [5]. The theory predicts that the branching ratio of  $\tau^- \rightarrow \omega \pi^+ \pi^- \pi^- \nu_\tau$  is about the same as that of  $\tau^- \rightarrow \omega \pi^- \pi^0 \pi^0 \nu_\tau$ .

As shown in Fig.1, there are many subprocesses in the decays. However, the calculation shows that the  $a_1$  meson (Fig.1(b)) dominates the two decay channels. If only the subprocess which is obtained from  $\mathcal{L}^{a_1\rho\pi}$  is kept in the matrix elements (15, 17), we obtain

$$B(\tau^- \rightarrow \omega\pi^-\pi^0\pi^0\nu_\tau) = 1.86 \times 10^{-4}, \quad (29)$$

$$B(\tau^- \rightarrow \omega\pi^-\pi^-\pi^+\nu_\tau) = 1.87 \times 10^{-4}. \quad (30)$$

86% of the decay rate comes from  $\mathcal{L}^{a_1\rho\pi}$ . It is necessary to point out that in Fig.1(b) there are terms which violate CVC. However, these terms are cancelled by the corresponding terms of other diagrams. The results(29, 30) are obtained after this cancellation. It is interesting to notice that  $a_1$  meson is associated with the  $a_1$  dominance in the axial-vector current [3].

The distribution functions of the two decay modes,  $\frac{d\Gamma}{dq^2}$ , are calculated and shown in Fig.2 and Fig.3. There is a peak in each distribution, which originates in the combination of the  $a_1$  resonance and the kinematics of the decays.

To conclude, two decay modes of  $\tau \rightarrow \omega\pi\pi\pi\nu$  have been studied by an effective large  $N_C$  QCD of mesons. CVC is satisfied in the chiral limit. Theoretical branching ratio of  $\tau^- \rightarrow \omega\pi^-\pi^0\pi^0\nu_\tau$  agrees with the data. The theory predicts that the branching ratio of  $\tau^- \rightarrow \omega\pi^+\pi^-\pi^-\nu_\tau$  is about the same as that of  $\tau^- \rightarrow \pi^-\pi^0\pi^0\nu_\tau$ . In this study there is no adjustable parameter.

## Appendix

### 1. diagrams involving the vertices (11-13)

$$\begin{aligned}
f_{12}(p_\rho) = & \frac{1}{2\pi^2 g^2} f_a^2 \frac{1}{m_a^4} \{-A(q^2, k_1^2) + k_1 \cdot p_1 B + k_1^2 D\} \\
& \times \{A(p_\rho^2, k_1^2) + k_1 \cdot p_2 B - k_1^2 D\} \\
& + \frac{1}{2\pi^2 g f_\pi} f_a \frac{1}{m_a^2} (1 - \frac{2c}{g}) \{-A(q^2, k_1^2) + k_1 \cdot p_1 B + k_1^2 D\} \\
& \times \{2F_1(-k_1 \cdot p_2) - k_1^2 F_2\} \\
& - \frac{1}{2\pi^2 g f_\pi} f_a (1 - \frac{2c}{g}) \frac{1}{m_a^2} \{A(p_\rho^2, k_1^2) + k_1 \cdot p_2 B - k_1^2 D\} \\
& \times \{2F_1(k_1 \cdot p_1) - k_1^2 F_2\} \\
& - \frac{1}{2\pi^2 f_\pi^2} (1 - \frac{2c}{g})^2 \{2F_1(k_1 \cdot p_1) - k_1^2 F_2\} \\
& \times \{2F_1(-k_1 \cdot p_2) - k_1^2 F_2\}, \tag{31}
\end{aligned}$$

where

$$\begin{aligned}
F_1(q_1 \cdot q_2) &= \frac{2}{g} \{1 + \frac{1}{\pi^2 f_\pi^2} q_1 \cdot q_2 [(1 - \frac{2c}{g})^2 - 4\pi^2 c^2]\}, \\
F_2 &= \frac{4}{f_\pi^2} [\frac{2c^2}{g} - \frac{3}{4\pi^2 g} (1 - \frac{2c}{g})^2 - \frac{1}{4\pi^2 g} (1 - \frac{2c}{g})]. \tag{32}
\end{aligned}$$

### 2. diagrams (Fig.1(c))

$$\begin{aligned}
f_{12}(p_\rho) = & -\frac{1}{k_1^2} \{-4F_1(k_1 \cdot p_1)F_1(-k_1 \cdot p_2) \\
& + 2k_1^2 F_2 F_1(-k_1 \cdot p_2) + 2k_1^2 F_2 F_1(k_1 \cdot p_1) - k_1^4 F_2^2\}. \tag{33}
\end{aligned}$$

3. diagrams (Fig.1(a))

$$\begin{aligned}
f(p_\rho) &= \frac{4}{f_\pi^2} \left\{ \frac{F^2}{g^2} - 2p_1 \cdot p_2 \left[ -\frac{2c^2}{g^2} + \frac{1}{4\pi^2 g^2} \left(1 - \frac{2c}{g}\right)^2 \right] \right. \\
&\quad \left. - \frac{3}{2\pi^2 g^2} \left(1 - \frac{2c}{g}\right) (p_2 \cdot p_\rho - q \cdot p_1) + \frac{k_1^2}{2\pi^2 g^2} \right\}, \\
f_{11}(p_\rho) &= -\frac{2}{\pi^2 g^2 f_\pi^2} \left(1 - \frac{2c}{g}\right), \\
f_{12}(p_\rho) &= -\frac{8}{f_\pi^2} \left\{ -\frac{2c^2}{g^2} + \frac{3}{4\pi^2 g^2} \left(1 - \frac{2c}{g}\right)^2 + \frac{3}{2\pi^2 g^2} \left(1 - \frac{2c}{g}\right) \right\}, \\
f_{21}(p_\rho) &= \frac{8}{f_\pi^2} \left\{ -\frac{4c^2}{g^2} + \frac{3}{4\pi^2 g^2} \left(1 - \frac{2c}{g}\right) \right\}, \\
f_{22}(p_\rho) &= f_{11}(p_\rho).
\end{aligned} \tag{34}$$

4. diagrams (Fig.1(d))

$$\begin{aligned}
BW &= \frac{1}{(p_1 + p_2)^2 - m_\rho^2 + i\sqrt{(p_1 + p_2)^2} \Gamma_\rho((p_1 + p_2)^2)}, \\
f(p_\rho) &= \frac{8}{g^2} BW q \cdot (p_2 - p_1) \left\{ 1 + \frac{p_1 \cdot p_2}{\pi^2 f_\pi^2} \left[ \left(1 - \frac{2c}{g}\right)^2 - 4\pi^2 c^2 \right] \right\}, \\
f_{12}(p_\rho) &= \frac{16}{g^2} BW \left\{ 1 + \frac{p_1 \cdot p_2}{\pi^2 f_\pi^2} \left[ \left(1 - \frac{2c}{g}\right)^2 - 4\pi^2 c^2 \right] \right\}, \\
f_{21}(p_\rho) &= -f_{12}(p_\rho).
\end{aligned} \tag{35}$$

The authors wish to thank M.Barnett. The study is supported by DOE grant No.DE-91ER75661.

## References

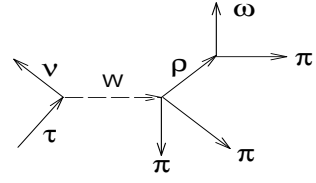
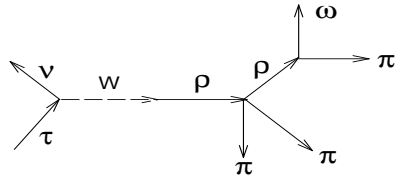
- [1] B. A. Li, Phys. Rev. D **52**, 5165 (1995), 5184 (1995).
- [2] D. N. Gao, B. A. Li, and M. L. Yan, Phys. Rev. D **56**, 4115 (1997 ); B. A. Li, D. N. Gao, and M. L. Yan, Phys. Rev. D **58**, 094031 (1998); J. Gao and B. A. Li, hep-ph/9911438, to appear in Phys. Rev. D.
- [3] B. A. Li, Phys. Rev. D **55**, 1436 (1997), 1425 (1997); Phys. Rev. D **57**, 1790 (1998).
- [4] D. Buskulic et al., ALEPH Collaboration, Z. Phys. C **70**, 579 (1996).
- [5] S. Anderson, Phys. Rev. Lett. **79**, 3814 (1997).
- [6] R. J. Bobie, Z. Phys. C **69**, 99 (1995).
- [7] A. Rouge, Z. Phys. C **70**, 65 (1996).
- [8] S. I. Eidelman and V. N. Ivanchenko, Nucl. Phys. **55C**(Proc. Supp l.), 181 (1997).
- [9] J. Wess and B. Zumino, Phys. Lett. B **37**, 95 (1971), E. Witten, Nucl. Phys. B **223**, 422 (1983).
- [10] J. J. Sakurai, Currents and Mesons, Univ. of Chicago Press, 1969.
- [11] Bing An Li, Phys. Rev. D **58**, 097302 (1998).

## Figure Captions

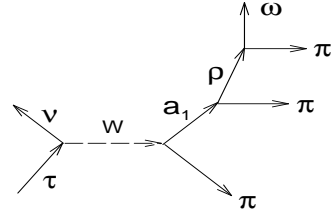
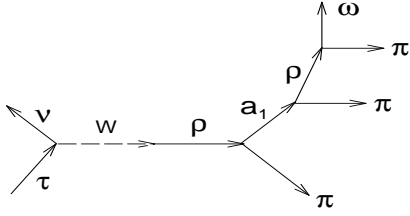
**FIG. 1.** Feynman Diagrams of  $\tau \rightarrow \omega \pi \pi \pi \nu$ .

**FIG. 2.** Distribution function  $\frac{d\Gamma}{dq^2}$  for  $\tau^- \rightarrow \omega \pi^+ \pi^- \pi^- \nu_\tau$ .

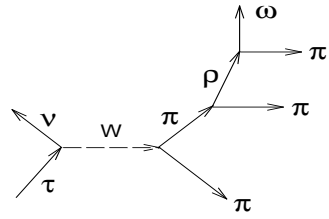
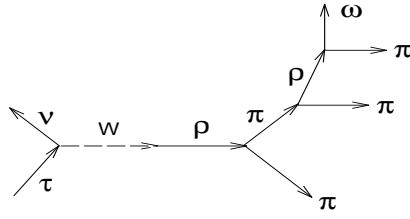
**FIG. 3.** Distribution function  $\frac{d\Gamma}{dq^2}$  for  $\tau^- \rightarrow \omega \pi^- \pi^0 \pi^0 \nu_\tau$ .



(a)

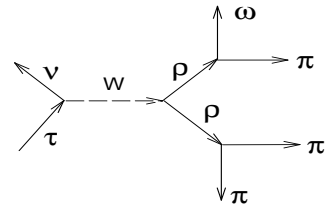
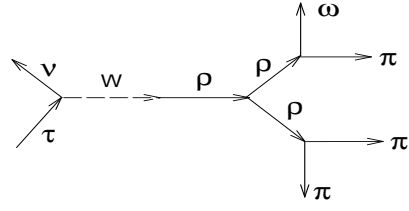


(b)

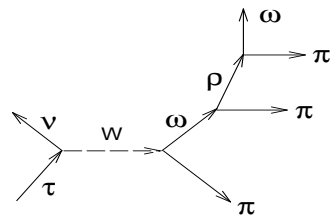
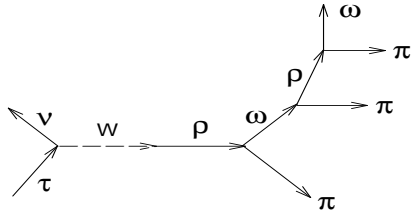


(c)

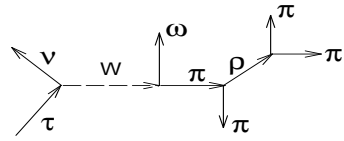
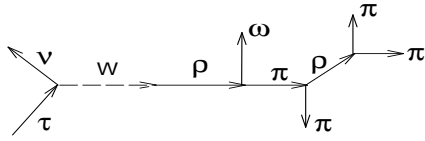
FIG. 1.



(d)



(e)



(f)

FIG. 1 cont'.



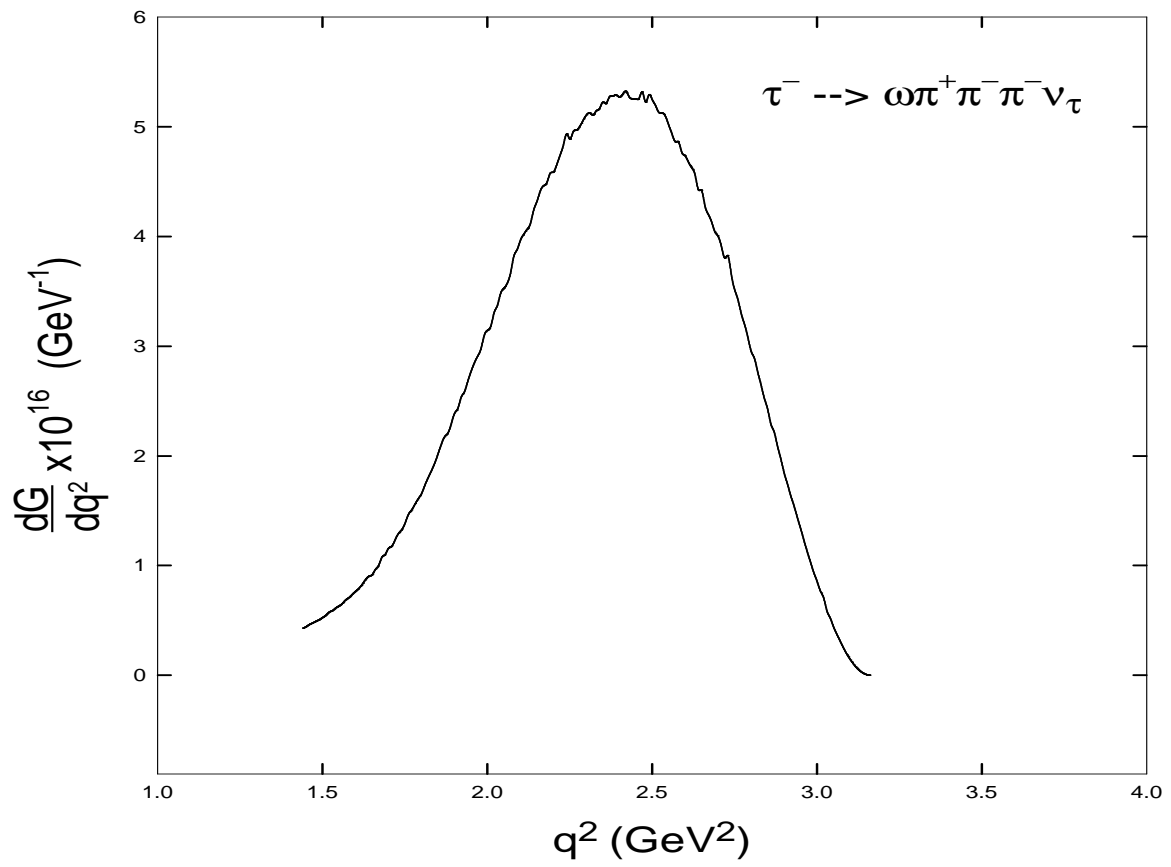


FIG. 2.

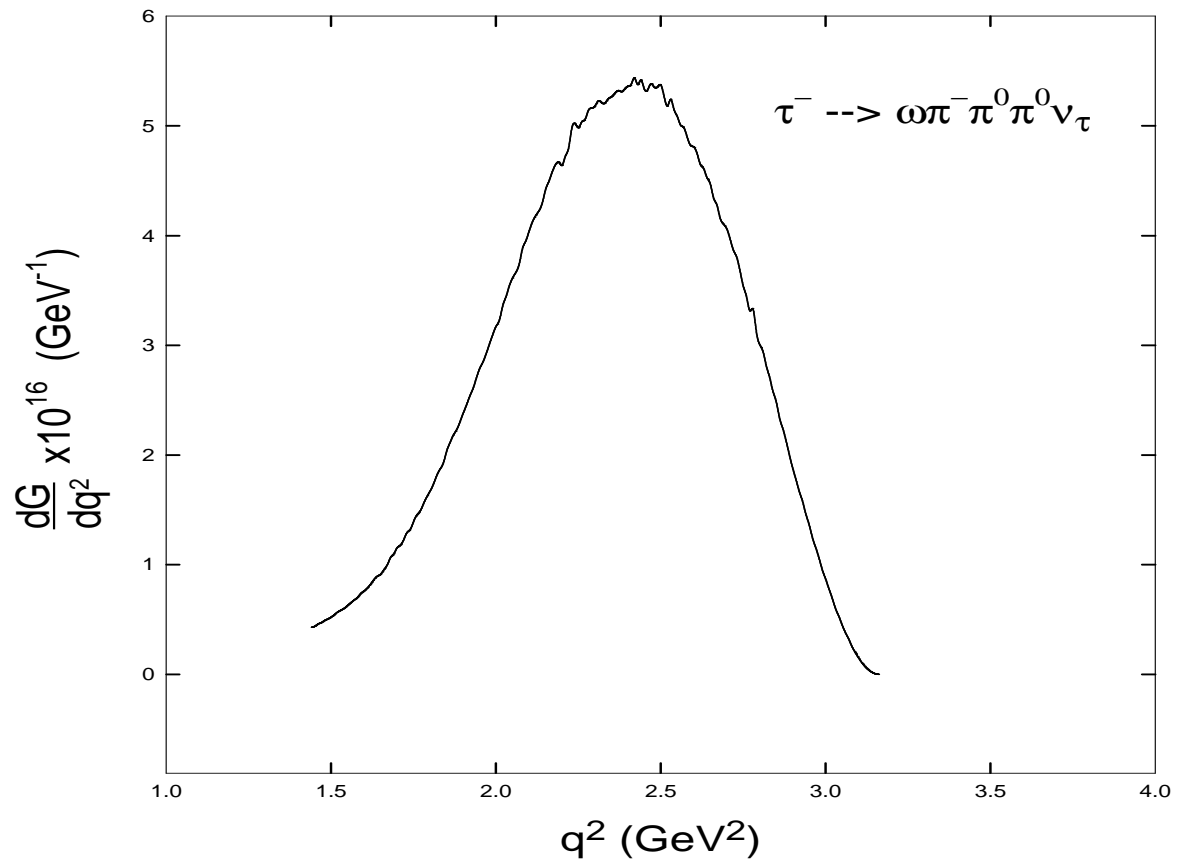


FIG. 3.